MyD88 innate immune function in a zebrafish embryo infection model

Sar, A.M. van der; Stockhammer, O.W.; Laan, C. van der; Spaink, H.P.; Bitter, W.; Meijer, A.H.

MyD88 Innate Immune Function in a Zebrafish Embryo Infection Model

Astrid M. van der Sar,[1] Oliver W. Stockhammer,[2] Carina van der Laan,[1] Herman P. Spaink,[2]
Wilbert Bitter,[1] and Annemarie H. Meijer[2]*

*Department of Medical Microbiology, VU Medical Centre, Van der Boechorststraat 7, 1081 BT Amsterdam, The Netherlands,[1]
and Institute of Biology, Leiden University, Wassenaarseweg 64, 2333 AL Leiden, The Netherlands[2]*

Innate immunity signaling mechanisms during vertebrate embryogenesis are largely unknown. To study Toll-like receptor (TLR) signaling function in the zebrafish embryo model, we designed an experimental setup for antisense morpholino knockdown under conditions of bacterial infection. Clearance of *Salmonella enterica* serovar Typhimurium Ra bacteria was significantly impaired after knockdown of myeloid differentiation factor 88 (MyD88), a common adaptor protein in TLR and interleukin-1 receptor signaling. Thereby, we demonstrate for the first time that the innate immune response of the developing embryo involves MyD88-dependent signaling, which further establishes the zebrafish embryo as a model for the study of vertebrate innate immunity.

Innate immunity relies heavily on signaling by members of the Toll-like receptor (TLR) family (25). TLRs and associated adaptor molecules are highly conserved between zebrafish (*Danio rerio*) and other vertebrates (13, 18). Bacterial and viral infections were found to induce expression levels of different zebrafish *TLR* genes (18, 20). However, direct functional evidence to confirm the role of TLR signaling in the innate immune response of zebrafish has not yet been reported.

The exploitation of zebrafish as an animal model for the study of immunity and infectious diseases is attractive for three main reasons (34, 28, 29, 30). First, high-throughput forward genetic screens in zebrafish are a powerful means to uncover novel immune functions. Second, the optical transparency of the free-living zebrafish embryos makes it possible to examine the early development of the immune system and the progression of microbial infections in real time (6, 11, 12, 31, 32). Third, the zebrafish embryo is easily accessible to experimental manipulations, and efficient inactivation of gene functions can be achieved by injection of antisense morpholino oligonucleotides (19). However, a major obstacle is that many of the immunological details and research tools that are available for more established animal models have not yet been resolved and developed for zebrafish.

The innate immune system of the zebrafish embryo starts developing during the first day postfertilization (dpf). Myeloid precursors originate from the anterior lateral plate mesoderm and migrate to the yolk sac, where they differentiate before the onset of blood circulation (11). Differentiated myeloid cells invade the head mesenchyme tissue or join the blood circulation (11, 12, 32). It has been shown that they are able to phagocytose apoptotic cell corpses (11). Furthermore, myeloid cells show specific adherence to bacteria injected into the blood and phagocytose them rapidly (6, 11, 31). They are also able to sense the presence of bacteria injected into one of the closed body cavities and to respond by migration to the infection site (11). All cells of the myeloid lineage initially express the transcription factor gene Pu.1 (Spi1), which is essential for their differentiation (21). After 1 dpf, Pu.1 expression decreases and two distinct populations of myeloid cells can be distinguished by the expression of two marker genes, *L-plastin*, which encodes a macrophage-specific actin-bundling protein, and *mpx*, which encodes a member of the myeloperoxidase family (3, 11, 17). At 2 dpf, the MPX-positive cells show the morphological characteristics of neutrophil granulocytes and are able to migrate to sites of trauma (4, 17). Immature lymphoblasts can first be detected by 3 dpf, but T and B lymphocytes do not mature until 4 to 6 weeks after hatching (5, 16). Therefore, the zebrafish embryo model is useful for determining the role of innate immunity in responses to different infectious agents, as it is uncoupled from adaptive immunity. With this approach, Davis et al. (6) showed that, during the first days of development, innate immunity determinants are sufficient for granuloma formation resulting from a mycobacterial infection.

To investigate the potential of the zebrafish embryo as a model for the study of vertebrate innate immune signaling, we first set out to determine the expression of *TLR* genes and associated adaptor genes during embryo development. Semiquantitative reverse transcription (RT)-PCR analysis, using the Superscript II one-step system (Invitrogen) with previously described conditions and primers (18), showed that at least 15 zebrafish *TLR* genes are expressed at 1 dpf, when the first functional macrophages and neutrophils enter blood circulation (Fig. 1). Most of these *TLR* genes are also maternally present, since expression was already detected at the 4-cell stage, which is prior to the onset of zygotic gene expression. Several *TLR* genes display distinct differential expression patterns during early stages of embryogenesis. For example, *zTLR1* expression peaks during the blastula and gastrula stages (dome to 80% epiboly) and is high during embryogenesis compared to the adult stage. Expression of *zTLR3* peaks during gastrulation and segmentation (80% epiboly to 5-somite stage), is reduced between 1 to 5 dpf, but returns to higher levels in the adult stage. Diffuse *zTLR3* expression in the developing brain of

* Corresponding author. Mailing address: Institute of Biology, Leiden University, Wassenaarseweg 64, 2333 AL Leiden, The Netherlands. Phone: 31 71 5274927. Fax: 31 71 5274999. E-mail: meijer@rulbim.leidenuniv.nl.
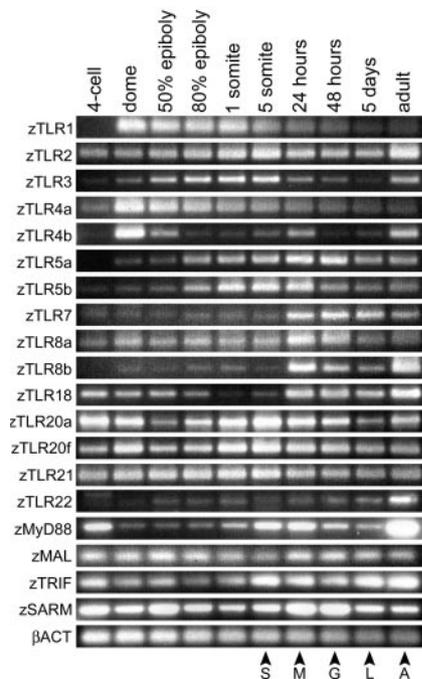
FIG. 1. RT-PCR analysis of zebrafish TLR and adaptor genes at different developmental stages. β-Actin (βACT) expression was determined for reference. One hundred nanograms of total RNA was used in the RT-PCR mixtures, except for zTRIF and βACT, where 50 ng was used. Forty cycles of amplification were used in all cases. The timing of development of the zebrafish immune system is indicated with marked arrow heads: S, hematopoietic stem cells can be distinguished in the ventrolateral mesoderm; M, embryonic macrophages migrate over the yolk sac, enter blood circulation, and are able to phagocytose injected bacteria; G, cells with typical granulocyte morphology can be distinguished that are able to localize to sites of acute inflammation; L, immature lymphoblasts can be detected and myelopoiesis is taken over by the anterior kidney; A, adaptive immunity is matured after 4 to 6 weeks of development.

zebrafish embryos was previously reported (20). A peak in the expression of *zTLR5a*, *zTLR5b*, *zTLR7*, *zTLR8a*, *zTLR8b*, and *zTLR18* coincides with the appearance of embryonic macrophages at 1 dpf. Expression of the *zMyD88* adaptor gene is highest in adults. In the embryo, maternal *zMyD88* transcript levels are reduced during blastula and gastrula stages and return to higher levels during segmentation and later stages (Fig. 1). The other MyD88 (myeloid differentiation factor 88)-like adaptor genes *zMAL*, *zTRIF*, and *zSARM* are also maternally present and expressed throughout embryogenesis (Fig. 1).

To study innate immunity signaling function in the zebrafish embryo, we targeted MyD88, which is known to function as a common adaptor protein in the downstream signaling pathways of all mammalian TLRs, except TLR3, and as an adaptor of the interleukin-1 and -18 receptors that are activated through TLR signaling (1, 2, 7). A morpholino knockdown approach (19) was used to interfere with MyD88 function by inhibition of its mRNA translation. An antisense morpholino (GeneTools) (5′-TAGCAAAACCTCTGTTATCCAGCGA-3′) was designed, which targets the leader sequence of the *zMyD88* mRNA (GenBank accession no. DQ100359) at positions −30 to −7 with respect to the ATG. A 5-bp mismatch control morpholino was used with the sequence 5′-TAcCAtAACCTg
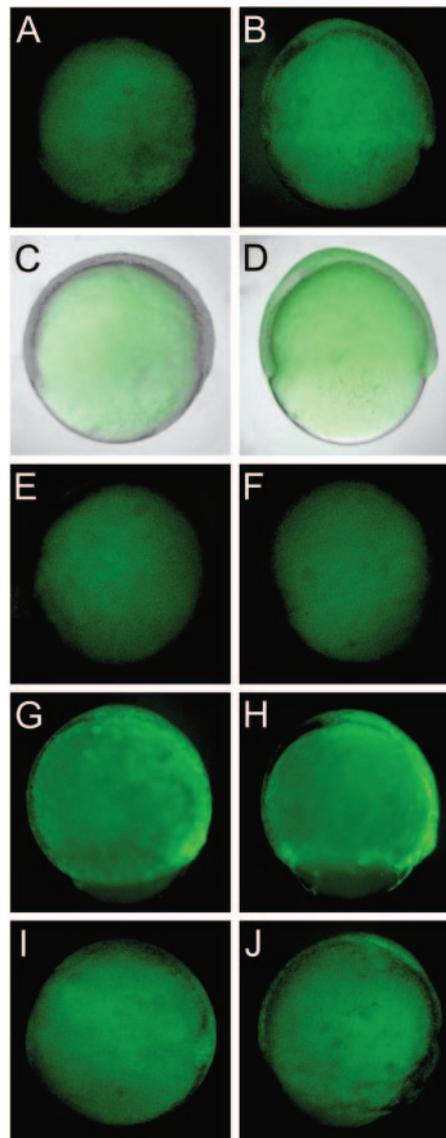

FIG. 2. Specificity of the MyD88 and 5-bp mismatch control morpholino. Embryos were injected with 2 ng of MyD88 morpholino (A, C, E, G, I) or with 2 ng of 5-bp mismatch control morpholino (B, D, F, H, J). (A, B) Coinjection of MyD88 (A) or mismatch (B) morpholino with 2 pg of *zMyD88-GFP* mRNA, which includes the 5′ leader sequence at which the morpholino is targeted. (C, D) Overlay of the fluorescence images from panels A and B with bright-field images of the same embryos. Note the absence of green fluorescent protein (GFP) signal in the embryonic tissues of the embryo coinjected with the MyD88 morpholino (A, C) and the presence of GFP signal in the embryonic tissues of the embryo coinjected with the mismatch control morpholino (B, D). The yolk shows autofluorescence independent of injection of the GFP construct. (E, F) Control embryos injected with MyD88 (E) or mismatch (F) morpholinos only, showing similar yolk autofluorescence as the embryo in panel A. (G, H) Coinjection of MyD88 (G) or mismatch (H) morpholino with 2 pg of *GFP* mRNA. (I, J) Coinjection of MyD88 (I) or mismatch (J) morpholino with 2 pg of a modified *zMyD88-GFP* mRNA lacking the morpholino target site. Note that fluorescence in the embryonic tissues of the embryos shown in panels G to J is unaffected by injection of the different morpholinos. Fluorescence images were acquired with a Leica DC500 camera and MZ Fluo 3 stereomicroscope. Fluorescence recordings were made with a fixed exposure time of 10.4 s and with the gain set at 1. Contrast was enhanced by 70% during image processing with Adobe Photoshop 6.0.
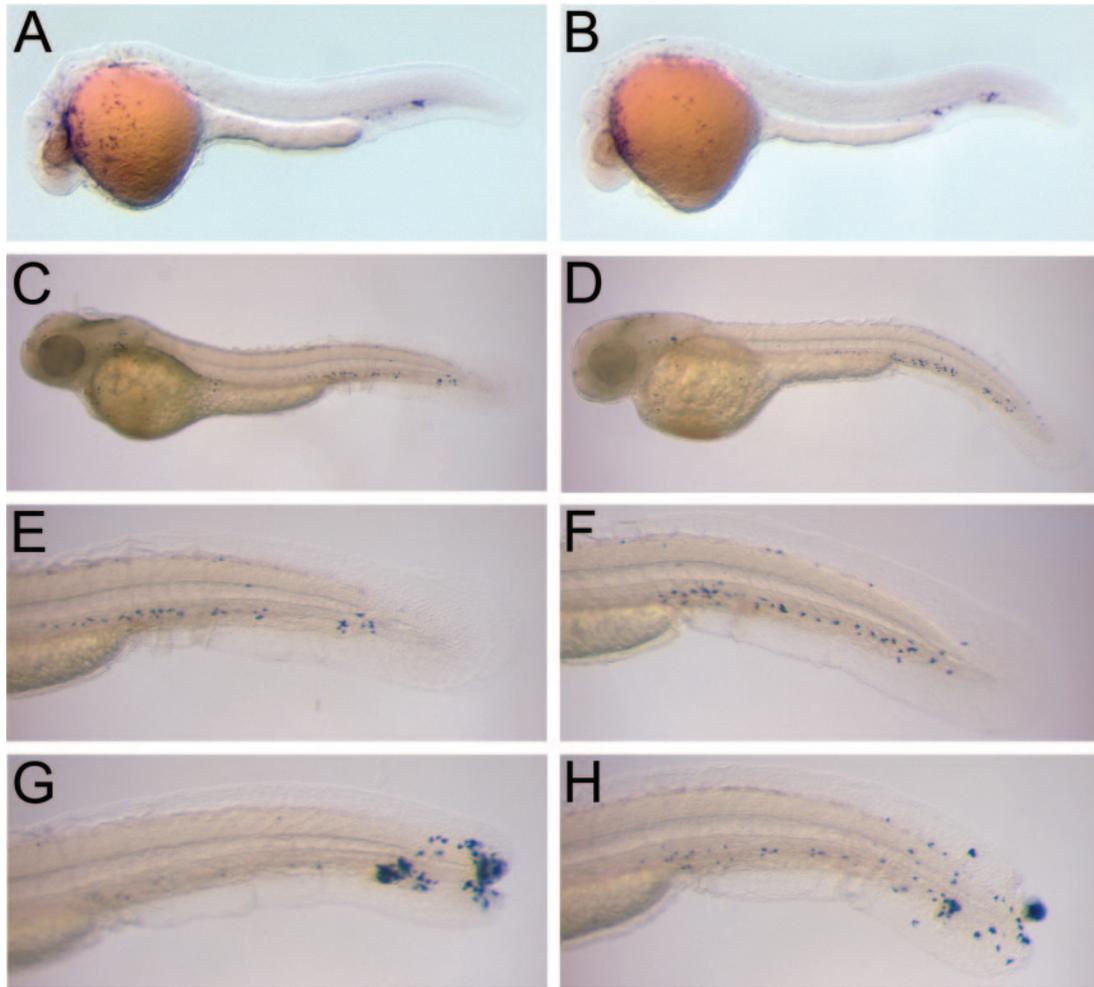
FIG. 3. Development and properties of myeloid cells in MyD88 morphants. Embryos injected with 1.7 ng of MyD88 morpholino (A, C, E, G) or with 1.7 ng of 5-bp mismatch control morpholino (B, D, F, H) were analyzed for L-plastin expression in macrophages (A, B) and for myeloperoxidase activity in granulocytes (C to H). (A, B), 1 dpf embryos; (C, D), 2 dpf embryos; (E, F) tails of the embryos shown in panels C and D; (G, H) tails of 2-dpf embryos analyzed 6 h after wounding of the tail fin. Embryos were grown in 0.003% 1-phenyl-2-thiourea (Sigma) to prevent melanization. Composite images were made of different focal planes.

TGTTATCgAGgGA-3′ (mismatches in lower case). For microinjection, morpholinos were diluted to different concentrations in Danieu's buffer (19), and approximately 1 nl was injected into the blastomere of the 1- to 2-cell stage embryo. To test the specificity of the MyD88 morpholino and its 5-bp mismatch control sequence, each of these morpholinos was first coinjected with a *zMyD88-GFP* fusion mRNA including the 5′ leader sequence. Embryos coinjected with the 5-bp mismatch control morpholino and *zMyD88-GFP* mRNA showed clear fluorescence at the 70 to 90% epiboly stage (Fig. 2B and D). In contrast, embryos coinjected with the MyD88 morpholino and *zMyD88-GFP* mRNA showed only autofluorescence of the yolk (Fig. 2A and C), similar to embryos injected with morpholinos only (Fig. 2E and F). Therefore, the MyD88 morpholino effectively blocks translation of *zMyD88-GFP* mRNA. Coinjection of each of the morpholinos with *GFP* mRNA (Fig. 2G and H) or with a modified *zMyD88-GFP* mRNA lacking the 5′ leader sequence (Fig. 2I and J) resulted in similar fluorescence levels in embryo tissues, confirming that

the MyD88 morpholino specifically targets the *zMyD88* leader sequence.

Embryos injected with 1.7 to 5 ng of MyD88 or control morpholinos showed no apparent morphological differences from wild-type embryos. To determine if myelopoiesis was affected in MyD88 morphants, we analyzed the expression of myeloid cell markers. From 1 dpf onwards, all myeloid cells of zebrafish embryos express either one of the two markers, *L-plastin* or *mpx* (3, 4, 11, 17). Expression of the macrophage marker gene, *L-plastin*, was examined at 1 dpf, after the onset of blood circulation. To this extent, a digoxigenin-labeled antisense riboprobe was synthesized with T7 RNA polymerase from an EcoRI-linearized *L-plastin* cDNA clone (GenBank accession no. AF157110), and whole-mount in situ hybridization was carried out according to the protocol of Thisse et al. (27). In MyD88 morphants, *L-plastin*-positive macrophages were dispersed over the yolk sac and some had accumulated in the ventral venous plexus (Fig. 3A). This pattern was similar to that observed in mismatch control morphants (Fig. 3B) and to the
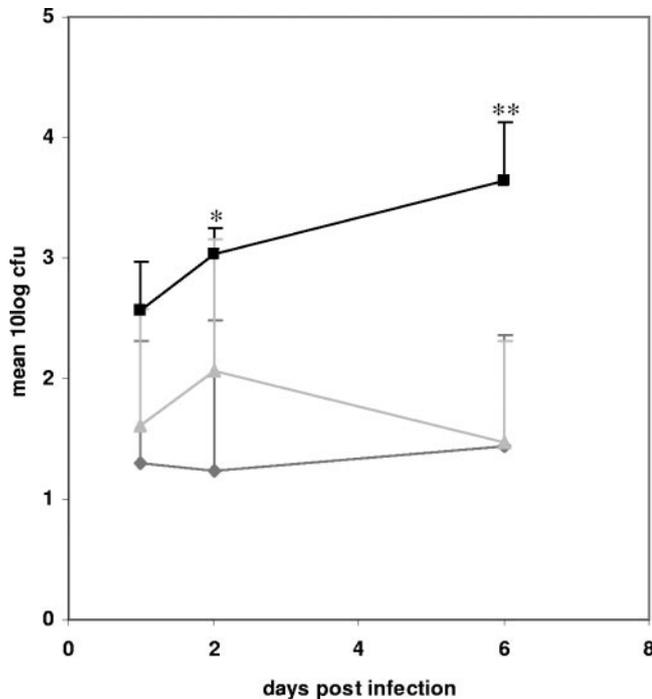
FIG. 4. Number of CFU of *S. enterica* serovar Typhimurium Ra isolated from infected wild-type (◆), mismatch (▲), and MyD88 morphant (■) embryos at different time points (dpi). Groups of 5 embryos were analyzed at each time point, and the mean 10log CFU value are presented on the graph. The numbers are the averages of results from four independent experiments. Statistical analyses were performed with single-factor analysis of variance tests and indicated that the difference between total CFU in wild-type and morphant embryos was significant at P values of <0.05 (∗) at 2 dpi and <0.01 (∗∗) at 6 dpi. The difference between total CFU in mismatch and morphant embryos was also significant at a P value of <0.01 (∗∗) at 6 dpi.

reported *L-plastin* expression pattern of wild-type zebrafish embryos (11).

A histochemical staining for myeloperoxidase (MPX) activity (17) was performed to check for the presence of granulocytes in embryos at 2 dpf. Peroxidase-positive cells in both the MyD88 and control morphants were abundantly present in the ventral venous plexus, and some were scattered over the yolk surface or had invaded the head region (Fig. 3C to F). The same distribution pattern of granulocytes was observed in noninjected control embryos (data not shown) and has been previously reported, based on both peroxidase staining and *mpx* gene expression (3, 17). Next, we took advantage of an acute inflammation assay devised by Lieschke et al. (17) to determine if the granulocytes of MyD88 morphants were functional. After wounding of the caudal fin with a sharp forceps, peroxidase-positive granulocytes of both MyD88 and control morphants accumulated at the site of trauma within 6 h, indicating their functional involvement in acute inflammation (Fig. 3G and H). In conclusion, based on *L-plastin* and MPX marker analyses, MyD88 morphants showed no apparent myelopoietic defects.

To demonstrate a function for MyD88 in the innate immune response of the zebrafish embryo, we made use of a *Salmonella enterica* serovar Typhimurium infection model that was previously established (31). In this infection model, a low dose of DsRed-labeled bacteria is injected into the embryo's bloodstream just after the onset of circulation at 1 dpf. While injection of the wild-type *S. enterica* serovar Typhimurium strain SL1027 resulted in a rapid lethal infection, its isogenic lipopolysaccharide (LPS) derivative SF1592 (Ra-type LPS mutant) proved to be nonpathogenic (31). In the present study, wild-type embryos, embryos injected with 1.7 ng of MyD88 morpholino, and embryos injected with the control morpholino were challenged in an infection experiment with *S. enterica* serovar Typhimurium Ra mutant bacteria containing the
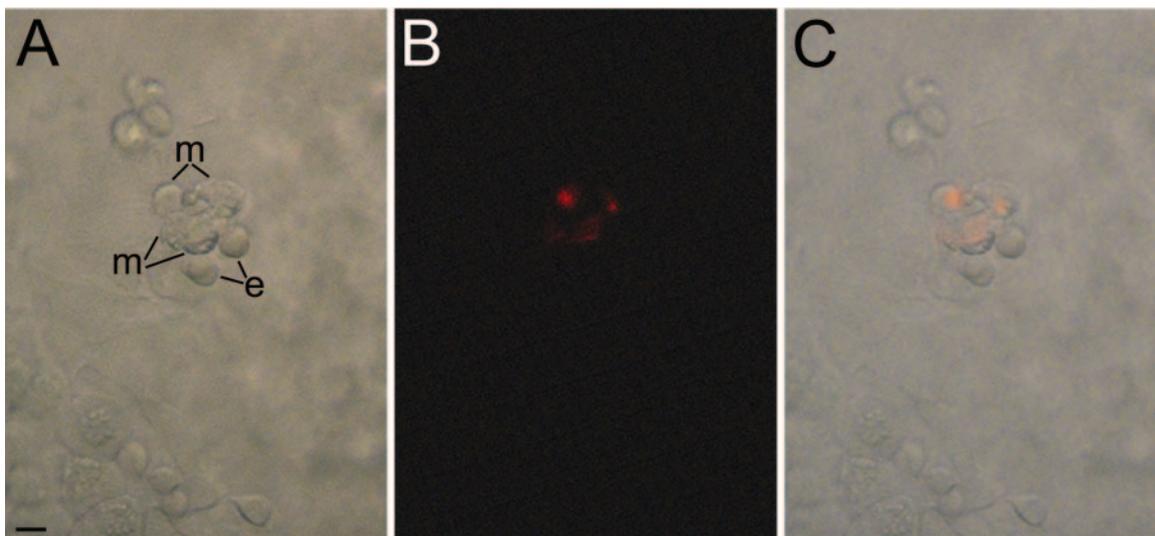

FIG. 5. Presence of *S. enterica* serovar Typhimurium Ra bacteria inside macrophages of a MyD88 morphant embryo. MyD88 morphant embryos were infected at 28 hpf by injection of DsRed-expressing *S. enterica* serovar Typhimurium Ra bacteria into the axial vein, and images of infected macrophages in the yolk sac circulation valley were taken after 1 h using a Leica DC500 camera and MZ 16 FA microscope. (A) Bright-field image showing a group of macrophages (m) and erythrocytes (e). (B) Fluorescence image of *S. enterica* serovar Typhimurium Ra in the same location as the macrophages. (C) Overlay image of panels A and B, indicating the ability of macrophages of MyD88 morphants to phagocytose bacteria. Scale bar, 10 μm.

DsRed plasmid pGMDs3 (31). Embryos were staged at 28 hpf (15) and individually infected by microinjection of approximately 100 CFU into the axial vein near the blood island and the urogenital opening as previously described (31). As a control, a similar dose as used in the infection experiment was spotted onto LB agar plates for CFU counting.

Embryos were monitored daily until 6 days after infection with *S. enterica* serovar Typhimurium Ra. No differences in survival rate were found between the infected wild-type embryos and MyD88 morphants. However, when embryos were examined for the presence of fluorescent bacteria, the MyD88 morphants showed more red spots, representing bacteria, than the wild-type embryos (data not shown). Therefore, total CFU counts were analyzed from groups of five embryos that were sampled at 1, 2, and 6 days postinfection (dpi). The pooled embryos were disintegrated (31), and the mixture was plated on LB agar plates. Four independent infection experiments were performed. At 1 dpi, the average number of total CFU was approximately fivefold higher in the MyD88 morphants than in wild-type and mismatch control embryos (Fig. 4). At 2 dpi, the difference between MyD88 morphants and wild-type embryos was 10-fold and significant at a P value of <0.05. Although it is not likely that morpholino knockdown is completely penetrant after 3 days of embryo development (19), a further increase of total CFU was still observed in MyD88 morphants at 6 dpi. At this stage, the difference with total CFU in wild-type and mismatch control embryos was significant at a P value of <0.01. Between different experiments, MyD88 morphant embryos harbored 100- to 1,000-fold more bacteria than wild-type and mismatch control embryos, which had either completely cleared the infection or contained only low amounts of bacteria not higher than the inoculum size (Fig. 4). Therefore we conclude that MyD88 morphants are not able to clear an infection with *S. enterica* serovar Typhimurium Ra effectively.

Although there was a clear increase in CFU counts, it is interesting that infection with the normally nonpathogenic LPS Ra mutant of *S. enterica* serovar Typhimurium was not lethal for MyD88 morphant embryos, indicating that multiplication of *S. enterica* serovar Typhimurium Ra is not completely uncontrolled in MyD88 morphant embryos. Future analysis of a stable MyD88 knockout line should clarify if this was due to incomplete loss of MyD88 function in morphant embryos or due to MyD88-independent innate immunity mechanisms.

To investigate if the inability of MyD88 morphants to clear *S. enterica* serovar Typhimurium Ra bacteria could be due to a defect in phagocytosis, embryos were examined at 1 h postinfection with a Leica MZ 16 FA microscope. DsRed-labeled bacteria were observed inside macrophages of MyD88 morphants (Fig. 5), similar to wild-type embryos or embryos injected with the mismatch control morpholino. Although we cannot yet exclude differences in phagocytosis efficiency or phagosome maturation, our present observations suggest that MyD88 morphants are primarily affected in activation of the bacterial killing mechanisms.

In conclusion, we have shown that TLR genes are broadly expressed during zebrafish embryo development and that MyD88 is required for a wild-type response of zebrafish embryos to *S. enterica* serovar Typhimurium Ra infection. These results indicate that MyD88-dependent signaling functions and is important in the early innate immune responses of embry-

onic zebrafish, independent from coupling to adaptive signaling responses. Furthermore, we have shown that zebrafish embryos express other MyD88-like adaptor molecules, such as Mal, TRIF, and SARM, suggesting that MyD88-independent signaling pathways also exist in zebrafish, similar to other vertebrates (8, 14, 33). The critical role of zebrafish MyD88 is consistent with many infection studies in MyD88$^{-/-}$ adult mice, which showed increased susceptibility to a variety of pathogens (9, 10, 22, 23, 24, 26). Therefore, the present study validates the zebrafish embryo as a useful model for analysis of the vertebrate innate immune system, which creates exciting possibilities for future studies in zebrafish embryo infection models.

REFERENCES

1. **Adachi, O., T. Kawai, K. Takeda, M. Matsumoto, H. Tsutsui, M. Sakagami, K. Nakanishi, and S. Akira.** 1998. Targeted disruption of the *MyD88* gene results in loss of IL-1- and IL-18-mediated function. Immunity **9:**143–150.
2. **Akira, S., and K. Takeda.** 2004. Toll-like receptor signalling. Nat. Rev. Immunol. **4:**499–511.
3. **Bennett, C. M., J. P. Kanki, J. Rhodes, T. X. Liu, B. H. Paw, M. W. Kieran, D. M. Langenau, A. Delahaye-Brown, L. I. Zon, M. D. Fleming, and A. T. Look.** 2001. Myelopoiesis in the zebrafish, *Danio rerio*. Blood **98:**643–651.
4. **Crowhurst, M. O., J. E. Layton, and G. J. Lieschke.** 2002. Developmental biology of zebrafish myeloid cells. Int. J. Dev. Biol. **46:**483–492.
5. **Davidson, A. J., and L. I. Zon.** 2004. The 'definitive' (and 'primitive') guide to zebrafish hematopoiesis. Oncogene **23:**7233–7246.
6. **Davis, J. M., H. Clay, J. L. Lewis, N. Ghori, P. Herbomel, and L. Ramakrishnan.** 2002. Real-time visualization of mycobacterium-macrophage interactions leading to initiation of granuloma formation in zebrafish embryos. Immunity **17:**693–702.
7. **Dunne, A., and L. A. O'Neill.** 2003. The interleukin-1 receptor/Toll-like receptor superfamily: signal transduction during inflammation and host defense. Sci. STKE **2003:**re3.
8. **Dunne, A., and L. A. O'Neill.** 2005. Adaptor usage and Toll-like receptor signaling specificity. FEBS Lett. **579:**3330–3335.
9. **Edelson, B. T., and E. R. Unanue.** 2002. MyD88-dependent but Toll-like receptor 2-independent innate immunity to *Listeria*: no role for either in macrophage listericidal activity. J. Immunol. **169:**3869–3875.
10. **Feng, C. G., C. A. Scanga, C. M. Collazo-Custodio, A. W. Cheever, S. Hieny, P. Caspar, and A. Sher.** 2003. Mice lacking myeloid differentiation factor 88 display profound defects in host resistance and immune responses to *Mycobacterium avium* infection not exhibited by Toll-like receptor 2 (TLR2)- and TLR4-deficient animals. J. Immunol. **171:**4758–4764.
11. **Herbomel, P., B. Thisse, and C. Thisse.** 1999. Ontogeny and behaviour of early macrophages in the zebrafish embryo. Development **126:**3735–3745.
12. **Herbomel, P., B. Thisse, and C. Thisse.** 2001. Zebrafish early macrophages colonize cephalic mesenchyme and developing brain, retina, and epidermis through a M-CSF receptor-dependent invasive process. Dev. Biol. **238:**274–288.
13. **Jault, C., L. Pichon, and J. Chluba.** 2004. Toll-like receptor gene family and TIR-domain adapters in *Danio rerio*. Mol. Immunol. **40:**759–771.
14. **Kaisho, T., O. Takeuchi, T. Kawai, K. Hoshino, and S. Akira.** 2001. Endotoxin-induced maturation of MyD88-deficient dendritic cells. J. Immunol. **166:**5688–5694.
15. **Kimmel, C. B., W. W. Ballard, S. R. Kimmel, B. Ullmann, and T. F. Schilling.** 1995. Stages of embryonic development of the zebrafish. Dev. Dyn. **203:**253–310.
16. **Lam, S. H., H. L. Chua, Z. Gong, T. J. Lam, and Y. M. Sin.** 2004. Development and maturation of the immune system in zebrafish, Danio rerio: a gene expression profiling, in situ hybridization and immunological study. Dev. Comp. Immunol. **28:**9–28.
17. **Lieschke, G. J., A. C. Oates, M. O. Crowhurst, A. C. Ward, and J. E. Layton.** 2001. Morphologic and functional characterization of granulocytes and macrophages in embryonic and adult zebrafish. Blood **98:**3087–3096.

18. **Meijer, A. H., S. F. G. Krens, I. A. Medina Rodriguez, S. He, W. Bitter, B. E. Snaar-Jagalska, and H. P. Spaink.** 2004. Expression analysis of the Toll-like receptor and TIR domain adaptor families of zebrafish. Mol. Immunol. **40:**773–783.

19. **Nasevicius, A., and S. C. Ekker.** 2000. Effective targeted gene 'knockdown' in zebrafish. Nat. Genet. **26:**216–220.

20. **Phelan, P. E., M. T. Mellon, and C. H. Kim.** 2005. Functional characterization of full-length TLR3, IRAK-4, and TRAF6 in zebrafish (*Danio rerio*). Mol. Immunol. **42:**1057–1071.

21. **Rhodes, J., A. Hagen, K. Hsu, M. Deng, T. X. Liu, A. T. Look, and J. P. Kanki.** 2005. Interplay of Pu. 1 and Gata1 determines myelo-erythroid progenitor cell fate in zebrafish. Dev. Cell **8:**97–108.

22. **Scanga, C. A., A. Bafica, C. G. Feng, A. W. Cheever, S. Hieny, and A. Sher.** 2004. MyD88-deficient mice display a profound loss in resistance to *Mycobacterium tuberculosis* associated with partially impaired Th1 cytokine and nitric oxide synthase 2 expression. Infect. Immun. **72:**2400–2404.

23. **Seki, E., H. Tsutsui, N. M. Tsuji, N. Hayashi, K. Adachi, H. Nakano, S. Futatsugi-Yumikura, O. Takeuchi, K. Hoshino, S. Akira, J. Fujimoto, and K. Nakanishi.** 2002. Critical roles of myeloid differentiation factor 88-dependent proinflammatory cytokine release in early phase clearance of *Listeria monocytogenes* in mice. J. Immunol. **169:**3863–3868.

24. **Skerrett, S. J., H. D. Liggitt, A. M. Hajjar, and C. B. Wilson.** 2004. Cutting edge: myeloid differentiation factor 88 is essential for pulmonary host defense against *Pseudomonas aeruginosa* but not *Staphylococcus aureus.* J. Immunol. **172:**3377–3381.

25. **Takeda, K., T. Kaisho, and S. Akira.** 2003. Toll-like receptors. Annu. Rev. Immunol. **21:**335–376.

26. **Takeuchi, O., K. Hoshino, and S. Akira.** 2000. Cutting edge: TLR2-deficient and MyD88-deficient mice are highly susceptible to *Staphylococcus aureus* infection. J. Immunol. **165:**5392–5396.

27. **Thisse, C., B. Thisse, T. F. Schilling, and J. H. Postlethwait.** 1993. Structure of the zebrafish snail1 gene and its expression in wild-type, spadetail and *no tail* mutant embryos. Development **119:**1203–1215.

28. **Traver, D., P. Herbomel, E. E. Patton, R. D. Murphey, J. A. Yoder, G. W. Litman, A. Catic, C. T. Amemiya, L. I. Zon, and N. S. Trede.** 2003. The zebrafish as a model organism to study development of the immune system. Adv. Immunol. **81:**253–330.

29. **Trede, N. S., D. M. Langenau, D. Traver, A. T. Look, and L. I. Zon.** 2004. The use of zebrafish to understand immunity. Immunity **20:**367–379.

30. **Van der Sar, A. M., B. J. Appelmelk, C. M. J. E. Vandenbroucke-Grauls, and W. Bitter.** 2004. A star with stripes: zebrafish as an infection model. Trends Microbiol. **12:**451–457.

31. **Van der Sar, A. M., R. J. P. Musters, F. J. M. Van Eeden, B. J. Appelmelk, C. M. J. E. Vandenbroucke-Grauls, and W. Bitter.** 2003. Zebrafish embryos as a model host for the real time analysis of *Salmonella typhimurium* infections. Cell. Microbiol. **5:**601–611.

32. **Willett, C. E., A. Cortes, A. Zuasti, and A. G. Zapata.** 1999. Early hematopoiesis and developing lymphoid organs in the zebrafish. Dev. Dyn. **214:**323–336.

33. **Yamamoto, M., K. Takeda, and S. Akira.** 2004. TIR domain-containing adaptors define the specificity of TLR signaling. Mol. Immunol. **40:**861–868.

34. **Yoder, J. A., M. E. Nielsen, C. T. Amemiya, and G. W. Litman.** 2002. Zebrafish as an immunological model system. Microbes Infect. **4:**1469–1478.

Editor: J. L. Flynn